CHAPTER THREE

EXPERIMENTAL TECHNIQUES

This chapter outlines the experimental techniques used in conducting the work presented in this thesis. Thin film deposition is an important aspect and is outlined in detail, with an emphasis on sputtering, which was the primary deposition method used, due to its potential as a scaleable thin film technique. Characterisation of the crystallographic texture was mainly by X-Ray diffraction, with a number of other techniques used to study the surface morphology and superconducting parameters.

3.1 An Introduction to Thin Film Deposition

3.1.1 The sputtering process

The basis of the sputtering process is the parallel plate glow discharge, shown schematically in figure 3.1. The anode is grounded and a large negative potential applied to the cathode. As the plasma formed between the plates has a very high conductivity the bulk of the applied voltage is dropped across the cathode, resulting in ion bombardment.

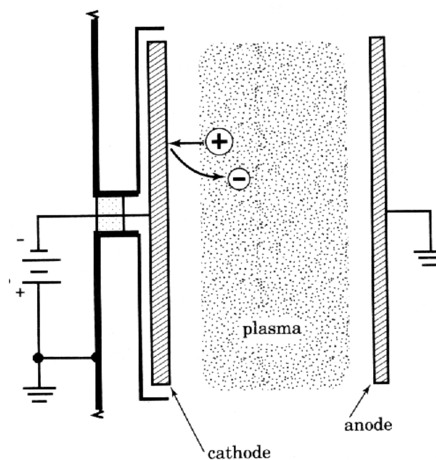

Figure 3.1 Parallel plate glow discharge from [205]

Ions which impinge on the cathode surface cause atoms to be ejected through a cascade process as indicated in figure 3.2. There are a number of other ion/surface interactions, one of which is the generation of secondary electrons. These electrons are accelerated into the plasma causing further ionising collisions, helping to sustain the process. However the majority of the electrons produced will not be involved in collisions but instead escape to the anode, making the process rather inefficient. The required gas pressure and applied voltage ranges required for the parallel plate glow discharge to be maintained are around 3-300 Pa and 1000-2000 V respectively.

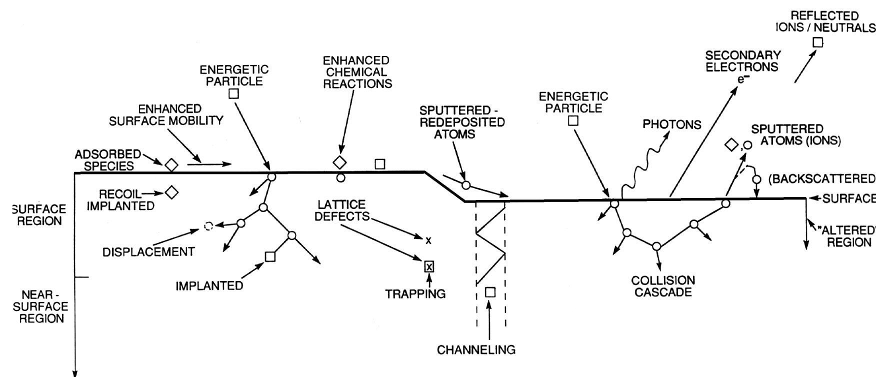

Figure 3.2 The sputtering cascade process (from [96]).

3.1.2 Magnetrons

In order to increase the efficiency of the sputtering process it is necessary to increase the number of collisions made by each secondary electron before it reaches the anode. This is done by applying a magnetic field in order to confine the electrons in orbits close to the cathode. The electrons are then subject to a Lorentz force in addition to that due to the electric field :

$$\mathbf{F} = -e(\mathbf{E} + \mathbf{v} \times \mathbf{B}), \tag{3.1}$$

There are a number of possible different magnetic field configurations, the most widely used being the planar magnetron, shown in figure 3.3. The bar magnets behind the target cause the magnetic field, emanating at right angles to the target, to bend so as to give a component

which is parallel to the target surface. Electrons which encounter this magnetron component of the field are subjected to a force tending to return them towards the target with a cycloidal motion. The arrangement of the magnets in the planar magnetron leads to a well defined region in which the electrons become confined. This region of the target, known as the 'racetrack', is heavily eroded due to the fact that there is greater ionisation of the gas directly above. Whilst the use of a magnetron significantly increases the rate at which a material may be sputtered, it also leads to less efficient use of the target material.

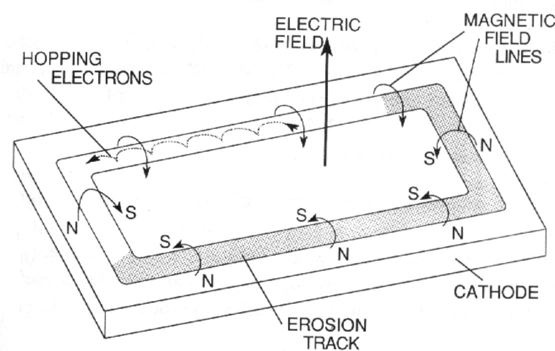

Figure 3.3 Schematic showing the effect of a planar magnetron (from [96]).

3.1.3 RF sputtering

If the cathode of figure 3.1 were replaced with an insulating material, the positive ions attracted to it would build up and eventually neutralise the target, preventing the attraction of further ions. Hence insulating materials may not be sputtered using the conventional DC method, instead an alternating current must be used. At low frequencies (less than about 50 kHz), the ions are sufficiently mobile that the electrodes simply alternate between being the anode and cathode. At greater frequencies however, two effects become apparent. Firstly the power may be transferred from the cathode through the insulating target by capacitive coupling. In addition, the electrons oscillating in the glow region become energetic enough to cause ionising collisions themselves, removing the need to maintain the secondary electrons in the cathode region. The standard rf frequency reserved for plasma processing is 13.56 MHz.

RF sputtering works by effectively self biasing the insulating target to a negative potential, so that it may be sputtered away by positive ion bombardment. This occurs because the grounded electrode (the substrates, shield and chamber walls) are far greater in area than the driven electrode (the target). The ion flux will be broadly uniform throughout the plasma and thus the target, being of small area will receive a smaller ion current. The electron current, however is determined by the plasma potential relative to the surface and is independent of surface area. Thus the target receives less ion current than electron current and is driven to a negative potential.

3.1.4 Reactive sputtering

It is possible to deposit an insulating film such as an oxide using DC sputtering if a metallic target is used with a reactive sputter gas (i.e. oxygen) instead of, or in addition to, the inert sputter gas (usually argon). Other compounds such as nitrides, carbides and sulphides may be deposited in this manner, using an appropriate reactive gas. Also it may be necessary to use a reactive sputter gas when depositing from an insulating target in order to control the stoichiometry of the deposited film.

One great advantage in depositing oxides from metallic targets through reactive sputtering is that it is much easier to produce a metallic target with a high purity. However, precise stoichiometric control may be difficult and can vary significantly with factors such as gas pressure and sputter rate. This rate is likely to be much less when reactively sputtering a target in a reactive gas than in an inert gas due to the fact that compounds form on the target surface.

3.1.5 Nucleation and growth

By placing a suitable substrate in the flux of atoms sputtered from the target surface, one can grow a thin film. When an atom or molecule arrives at the substrate it must be absorbed onto the surface, which is a two-stage process. The molecule approaches the substrate and interacts with atoms at the surface. If its momentum is dissipated during the interaction it may

no longer have enough energy to escape and will be physically trapped on the surface – this process is known as physisorption. The molecule is still able to diffuse across the surface and may either desorb if it gains sufficient energy, or it may interact with other surface atoms to form chemical bonds (chemisorption). The surface diffusion step is very important as it enables the adsorbed atoms to find low energy sites

Following initial nucleation there are three basic modes of film growth, depicted in two dimensions in figure 3.4. Layer (Frank – van der Merwe) growth occurs when the incoming atoms or molecule are attracted more strongly to the substrate than to each other and therefore complete an entire layer before starting to form a new one. This growth mode is favourable for the achievement of epitaxial growth. If the incoming atoms bond more strongly with each other than with the substrate, then island (Volmer-Weber) growth results with the atoms forming 3 dimensional nuclei. It is also possible that a mixture of the two modes may be seen, as the energy associated with successive layers changes. This leads to a mixed mode known as Stranski-Krastanov.

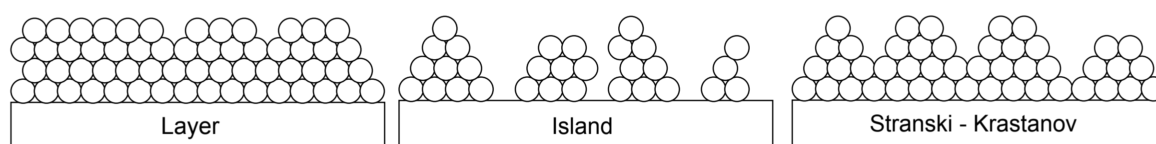

Figure 3.4 Illustration of the different thin film growth modes

3.1.6 Epitaxy

The term epitaxy refers to the process by which the crystallographic texture of a thin film is influenced by that of the substrate onto which it is deposited. When epitaxial growth is achieved, the film orientation is determined by matching of the lattices at the film/substrate interface. For different materials there will be some amount of mismatch which may be accommodated in a number of ways, as outlined in figure 3.5. In the case where the degree of mismatch is incredibly small, the interface will be effectively commensurate, with negligible strain required for matched growth (a). If however the lattice parameter of the film is significantly different (in this example, larger) than that of the substrate, the mismatch can be

accommodated in a number of ways. If bonding between the layers is very weak, the film may remain incommensurate and therefore unstrained. It is more likely however that the film and substrate will be chemically bonded, in which case, the film will either be strained as shown in (c) or relaxed, with dislocations (d). The smaller the degree of mismatch, the more likely it is that a strain can be tolerated without the introduction of dislocations. Calculations have shown that for a single monolayer, a strain of 9% may be tolerated for commensurate epitaxial growth to be stable (or metastably up to 14%) [206]. However the total amount of strain energy in the film will increase linearly with deposition of successive layers and hence there is a critical thickness at which dislocations must be introduced.

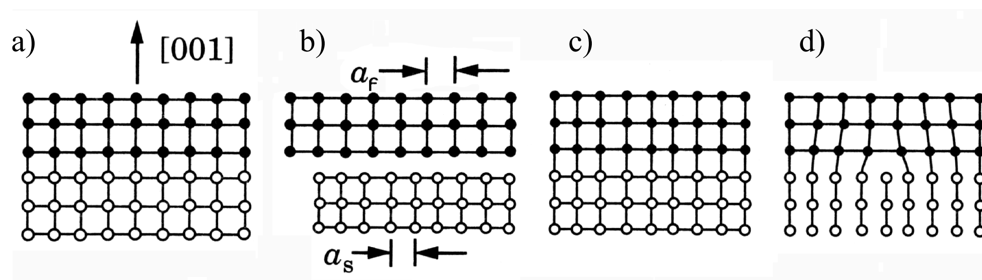

Figure 3.5 Schematic of the ways in which lattice mismatch between a film with lattice parameter a_f and substrate with lattice parameter a_s may be accommodated (from [205]).

Even if predictions based on lattice matching indicate that a particular epitaxial orientation may be favourable, whether it is achieved in practice will depend to some extent on the deposition parameters. Epitaxial growth requires that incoming atoms are sufficiently mobile that they can diffuse around on the surface in order to find low energy sites. Hence the achievement of epitaxy will generally be favoured by a low deposition rate and by a high substrate temperature.

3.2 Practical Thin Film Growth

3.2.1 Vacuum systems

An essential aspect of experimental apparatus involved in thin film deposition is the vacuum system, comprising a deposition chamber, gas reservoir, valves, gauges, pumps and

interconnecting piping. The deposition apparatus used to carry out the majority of the work described in this thesis was the Mark VI sputter system. A high vacuum is achieved through the use of two pumps, an Edwards rotary pump and an oil vapour diffusion pump. The diffusion pump cannot discharge directly to atmosphere, and so the rotary pump is used as a backing pump, maintaining a sufficiently low outlet pressure. The rotary pump is also used in order to rough the chamber to below about 0.1 Torr in order that the diffusion pump is not subjected to a large load.

There are 3 gas cylinders, containing argon, oxygen and hydrogen, each connected to a gas reservoir. This reservoir is connected to the chamber by a leak valve, allowing control of the gas flow rate. It was also possible to introduce the hydrogen directly to the chamber via an alternative leak valve. Pressure was monitored by the use of various gauges. Pirani pressure gauges were used to monitor the pressure in the chamber and at the back of the diffusion pump and baratron gauges were used to measure accurately the pressure in both the chamber and reservoir.

All UHV connections are made using knife edges and copper gaskets, in order to minimise leaks. It is however impossible to create a perfect seal and so in practice, one needs to keep the leak rate to a manageable level. A leak can be distinguished from outgassing from the chamber walls as the pressure rise associated with a leak is linear over time, whereas outgassing tends to saturate. Also, if the system is equipped with a mass spectrometer, a significant leak to atmosphere can be identified by observing the relevant proportions of gases in the air.

3.2.2 Magnetrons and shields

The magnetrons used consist of a $SmCo_5$ permanent magnet, separated from the magnetron body (mild steel) by an aluminium spacer. The magnetic field lines form closed paths and have typical field strengths of around 0.3 T parallel to the target surface. If the target material is a metal, it may simply be screwed to the magnetron, and the screw heads are then covered over with a thin foil of the target material. Shielding which is also made of the target material

is used to cover the body of the magnetron. These steps are taken in order to eliminate sputtering of impurity atoms from the magnetron itself.

The arrangement for a ceramic target is significantly different. Because it is impractical to drill holes into the target, it is held to the magnetron body with spring-steel clips. A further complication is that due to the fact that as the deposition mode is RF sputtering, the shield must be isolated from the target and grounded. The isolation is achieved through the use of PTFE screws and the grounding is via a thin wire connected to the flange. In order to prevent the magnetron reaching very high temperatures during deposition it is usually water cooled.

3.2.3 Targets

A number of different target materials were used during the course of this work. Metallic targets of Ni, Pd and Ag were obtained in sheet form, approximately 1 mm thick and holes were drilled in order to attach them to the magnetron. As sputtering occurs much faster in the racetrack region than elsewhere, the target is eroded through rather quickly. When this occurs more target material must be placed behind the racetrack in order to prevent sputtering of the magnetron itself.

Ceramic targets were produced by sintering oxide powders at approximately 1600ºC. The CeO_2 powder used was of 99.99% purity and the $ZrO_2/8\%Y_2O_3$ powder 99.9%. One CeO_2 target was purchased from Goodfellow Metals. These targets, approximately 2-3 mm thick were glued to a metallic backing plate using silver/epoxy glue in order to achieve good thermal and electrical contact between target and magnetron.

3.2.4 Substrate heating

A very simple heating arrangement is the metallic strip heater, made of platinum, which has a high melting point (1768ºC) and rather good high temperature oxidation resistance. It is approximately 0.1 mm thick and 10 mm wide and has edges folded up to form a shallow cavity. The strip is heated by the passing of a direct current through its length. Ceramic

substrates rest in the cavity and are heated by thermal conduction. If metallic tapes are placed on the heater the situation is complicated by generation of currents in the substrate itself. Therefore the tape is placed in thermal contact with a ceramic block, isolating it from the strip heater.

There are a number of practical problems associated with the strip heater making it very difficult to heat substrates uniformly and reproducibly. Firstly the temperature of the heater itself is not particularly uniform as there will inevitably be some oxidation of the Pt strip when in use, leading to changes in the emmisivity of the surface. This causes fluctuations in the temperature along the length of the heater so that if a number of substrates are placed on it during one run, they are unlikely to be at equal temperatures. Also thermal conduction between a metal strip and ceramic substrate, with essentially three points of mutual contact, is rather inefficient and thus the strip has to be heated to a much higher temperature than one requires at the substrate. The lack of control over contact also causes the surface temperature of individual substrates to be non-uniform.

A more practical heater particularly suitable for high temperature depositions has been designed and built by Mr G. Wagner [207]. It uses radiative coupling between the heater strip and substrates, which are several mm away, as shown in the schematic of figure 3.6. The heater strip itself is 50 µm thick, 90 mm long and 30 mm wide and is made from an Fe-Cr alloy. It is clamped between the contact blocks at each end and heated by a direct current of up to 50 A. Two Pt coated silica plates (50 mm square and 1-2 mm thick) are placed above and below the heating element. Each plate has a hole cut into it, the upper one having ledges on which the substrates rest. The lower plate may be used as a site for a “dummy” substrate to which a thermocouple may be welded, though this was not routinely done. Again this heater is designed for ceramic substrates and is not ideal for use with metallic substrates. Tapes may be clamped between the silica plates, but a large amount of heat is lost through conduction.

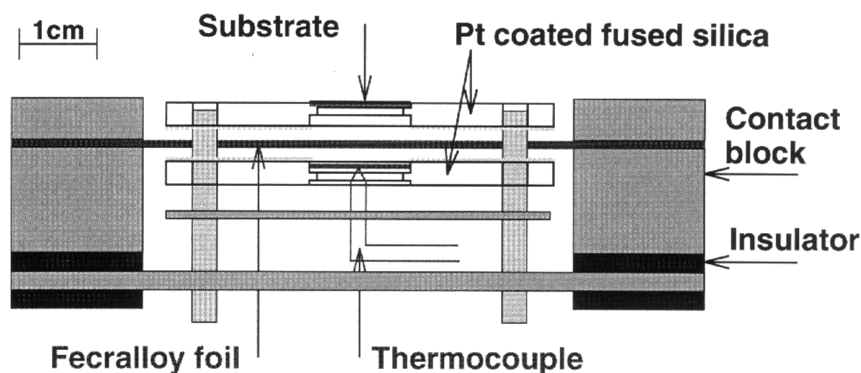

Figure 3.6 A schematic of the radiative heater (adapted from [207])

A simpler way to heat metallic tapes is to do so directly by passing a current along their length. The method is very efficient and potentially can be both controllable and reproducible. The temperature will not be uniform along the surface of the whole substrate, being significantly hotter in the centre due to the fact that heat is conducted away at the clamped ends. Ideally if identical tapes are used the temperature at any point on the surface can be easily reproduced by using the same heating current. The factors which will determine the temperature are tape dimensions, electrical resistance and surface emmisivity, which are approximately the same for each NiFe substrate at the beginning of each experiment. However, a complication is that the electrical resistance and the emmisivity may change during the course of a deposition run, which causes the temperature to change significantly also.

3.2.5 Temperature measurement

The operating temperature of a heater may be measured through the use of a thermocouple, usually welded to the heater surface. This can be done for both the strip heater and radiative heater but, as already mentioned, the difference between the heater and substrate temperature can be large and uncertain. Ideally one would attach a thermocouple to the substrate itself and perform a calibration, but the presence of the measuring device (particularly when used with thin metallic substrates) alters the substrate temperature.

Where it is possible to view the inside of the measuring chamber, through a window on the flange, an easier temperature measurement method is optical or infra-red pyrometry. In the majority of this work substrate temperatures were measured using a Heimann infra-red pyrometer, model KT 19.99, which detects wavelengths of 9.6-14.1 μm.

3.2.6 Deposition procedures

In order to remove dust from the surface of the substrates they must be cleaned before being loaded into the deposition system. MgO substrates were cleaned in chloroform, ultrasounding for 5 minutes, then dried in a flow of nitrogen gas. Other ceramic substrates such as silica and sapphire were cleaned in a similar manner, but using acetone rather than chloroform. The metallic tapes in short pieces may be cleaned in the same way, though longer lengths may suffer mechanical damage when ultrasounded and so were usually bathed in still acetone for approximately 10 minutes before drying in nitrogen.

If the strip or radiative heaters are used, the substrates are simply placed on the appropriate platform. An extra substrate may be included to act as a thickness monitor and by measuring the step height of this film, the film thickness (and hence deposition rate) can be determined. If a tape is to be heated directly, its ends are clamped firmly between two current contact blocks. It is possible to place up to 3 tapes alongside each other at one time and the tapes may be placed in tension if required.

The flange is loaded into the vacuum chamber and a seal made through a copper gasket between the knife edges. The chamber is then 'roughed' using a rotary pump, which reduces the pressure to approximately 0.1 Torr. At this point pumping is transferred to the diffusion pump in order to attain a high vacuum. The leak rate may be monitored by closing the gate valve and the pressure rise is likely to be high initially due to outgassing from the chamber walls and flange. In order to increase the rate of outgassing the system is usually 'baked out' for several hours, a process which involves heating the chamber walls to approximately 150ºC.

Ideally the sputter gases should be mixed in the reservoir before deposition, but when a number of different mixtures need to be used during one run, this may not be possible. Where a run required 3 stages, progressing from Ar/H_2 to pure Ar to Ar/O_2, Ar was placed in the reservoir initially. H_2 was piped directly into the chamber in stage 1, mixing with the Ar in the chamber. This flow was then stopped by closing the leak valve, to ensure pure Ar from the reservoir in stage 2, and then O_2 was mixed with the Ar in the reservoir to begin stage 3. In order to minimise impurities in the sputter gas, a flow of gas is maintained during deposition by opening the gate valve slightly. By adjusting the gate valve and reservoir leak valve, a reasonable flow rate is set up and the chamber pressure accurately controlled.

As well as establishing the appropriate chamber pressure, the substrates may need to be preheated prior to deposition. Also the target may need to be pre-sputtered for a short time in order to remove any impurities from its surface. Therefore the substrates are shielded from the target by inserting a physical barrier, or simply by rotating the substrates so that they are no longer beneath the magnetron. The magnetron cooling water is turned on and the discharge is then struck by turning on the magnetron power supply. It may be necessary to raise either the pressure or power in order to initiate the discharge before returning them to the required levels to carry out the deposition. Metals were usually deposited in pressures around 1 Pa and with DC power up to 25 W with typical values for ceramics of around 5 Pa and 30 W RF power.

3.3 X-Ray Diffraction

3.3.1 The Ward-Wallace camera

In 1975 Ward and Wallace introduced a method suitable for the X-ray texture analysis of thin films [208, 209]. A cylindrical camera with a standard diameter of 5.73 cm is loaded with photographic film and the specimen mounted on the camera axis as shown in figure 3.7. The sample is positioned such that the surface makes an angle i, from 0° to 39°, with the incident beam. Also the sample rotates in its own plane during exposure. The position of the specimen

along the axis of the camera is not crucial and by altering this, one may examine the high or low 2θ region.

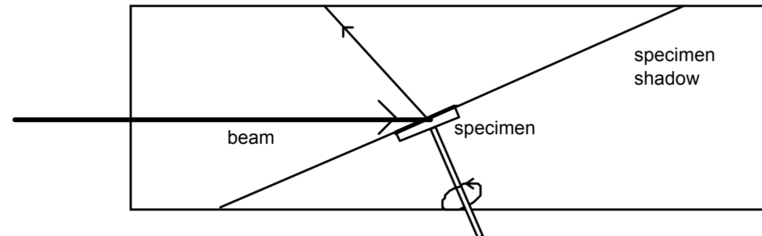

Figure 3.7 Schematic of the Ward-Wallace camera geometry

If the sample is a randomly oriented polycrystal the X-Rays are diffracted from planes of spacing *d* in cones of half angle 2θ, where θ is related to *d* and the X-Ray wavelength, λ, by the Bragg equation ;

$$\lambda = 2d \sin \theta \tag{3.2}$$

The intersection between the cones and the cylindrical film produces straight lines. The relationship between the distance along the film, *y*, and 2θ is given by

$$y = R \cot 2\theta \tag{3.3}$$

where *R* is the camera radius.

If the angle between a set of diffracting planes and substrate normal is ϕ, then the *x* co-ordinate recorded on the film due to reflections from those planes is given by $x=R\phi$. Not all the diffraction pattern will be visible on the photograph due to the specimen shadow. This shadow boundary is described by the intersection of the specimen plane and the cylindrical film and is described for an incident angle *i* by

$$y = R \cot i \cos (x/R) \tag{3.4}$$

$$\cos \phi = \tan i \cot 2\theta \tag{3.5}$$

When well oriented films are measured, only some parts of the diffraction cone will be present. If α is the angle between the specimen normal and the diffracting plane normal, the angles at which peaks are present are given by

$$\cos \alpha = \sin \theta \sin i + \cos \theta \cos i \cos \alpha \qquad (3.6)$$

There will, however be an upper and lower limit to the value of α which will be recorded. The upper limit is set by the region within the specimen shadow and is given by equation 3.4. The lower limit occurs when ϕ=0 and is described by equation 3.5. Hence

$$\cos \alpha_{max} = \sin i / (2 \sin \theta) \qquad (3.7)$$

$$\cos \alpha_{min} = | \theta - i | \qquad (3.8)$$

Usually an incidence angle *I,* of 30° is used and a standard grid onto which contours of equal θ and α are plotted may be used to index the photograph. Often however one will be in a position of knowing the identity of the material in question and can use equations 3.2 and 3.4 to calculate the expected positions of the peaks and then compare this to the photographic film.

The main advantage of this technique is that by using photographic film, diffracted X-Rays are detected over a 2-dimensional surface. In this way orientation information may be gathered from several sets of diffracting planes and possibly from several different layers simultaneously.

3.3.2 The vertical diffractometer

A Philips PW1710 vertical diffractometer with a Cu Kα X-Ray source was used to carry out θ-2θ scans and rocking curves. Samples are mounted on glass plates and clamped in place using a sprung clip. Sample height is controlled as shown in figure 3.8, using plasticine to ensure that the sample surface is at the same level as the top of the glass slide and hence coincident with the axis of rotation of the diffractometer. If the surface is displaced by a

distance *D*, from the centre of the diffractometer (of radius *R*), this will cause an error in 2θ, given by [210] :

$$\delta (2\theta) = 2D (\cos \theta) / R \quad (3.9)$$

hence a displacement of 0.1 mm causes an error in 2θ of 0.07° at 2θ=40°.

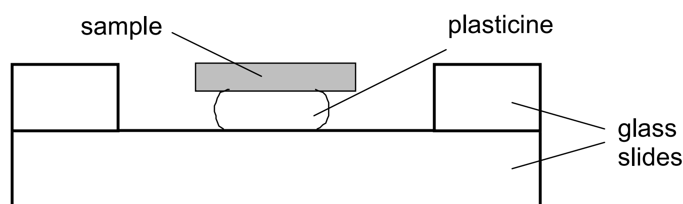

Figure 3.8 Method of mounting samples for X-Ray measurement in the vertical diffractometer

The choice of divergence and receiving slits is an important factor. Narrow slits give good resolution but irradiate a smaller area of the sample, which may turn out not be representative. In addition the intensity is reduced with the consequence that the counting time may have to be increased, although when measuring oriented samples, particularly single crystals, peak intensities are usually quite high. Table 3.1 indicates the length of the sample that is irradiated as a function of 2θ for various slit widths. It is crucial that the slits are chosen so that at the lowest 2θ, the irradiated length is not greater than that of the sample and that at the highest 2θ, the irradiated length contains sufficient grains to give a representative measurement.

Table 3.1 Irradiated X-ray length (in mm) at a given 2θ value for various widths

2θ Position (°)	Divergence Slit Width (°)				
	4	1	1/2	1/4	1/30
5	*277*	*69*	*35*	*17*	*2.3*
10	*139*	*35*	*17*	*9*	*1.2*
20	*70*	*17*	*9*	*4*	*0.6*
30	*47*	*12*	*6*	*3*	*0.4*
40	*35*	*9*	*4*	*2*	*0.3*
60	*24*	*6*	*3*	*1.5*	*0.2*
80	*19*	*5*	*2*	*1.2*	*0.2*
120	*14*	*3*	*2*	*0.9*	*0.1*

One use of the vertical diffractometer is to carry out a θ-2θ scan which involves coupling the rotation angle of the sample and detector in a 1:2 ratio whilst the position of the source beam remains fixed. In this way the angle made by the incident and detected beam with the sample surface, shown in figure 3.9, is θ. Because these angles are equal only planes which are parallel to the sample surface are detected using such a method. Note that it is possible to de-couple the 1:2 rotation ratio so the angles are no longer equal. In this case the angle between the incident beam and the sample surface is usually referred to as ω and the angle between incident and detected beam is still 2θ, as shown in figure 3.9.

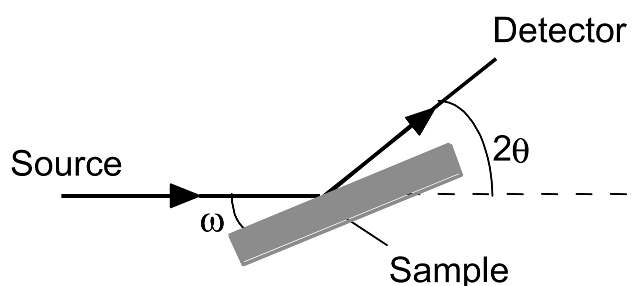

Figure 3.9 The set-up of the vertical diffractometer. By coupling ω and 2θ a goniometer scan may be carried out.

The decoupling of sample and detector angles can be used to carry out a rocking curve. The 2θ position of the relevant reflection from {hkl} planes parallel to the sample surface is located using a θ-2θ scan. The detector arm is then fixed whilst the sample is rotated in order to detect the reflection from planes with the same {hkl} indices which are in slightly different orientations.

3.3.3 The texture goniometer

The texture unit is a Philips X'Pert system with an Automated Texture Goniometer cradle. Samples are mounted on an aluminium mushroom stage and sample height is adjusted using a retractable needle as a guide. The detector arm and sample stage move in the same way as the vertical goniometer, hence the texture unit can be used to perform θ-2θ scans and rocking curves, although the resolution is not as good due to the different optical arrangement. The texture cradle which is mounted on the sample stage enables the sample to be rotated in the

plane which is normal to both its surface and the plane containing the incident X-Ray beam (ψ scan) and also in its own plane (ϕ scan). The ϕ scan may be measured over the entire 360° range, but the ψ scan is limited between –70° and +70° due to defocussing effects. By measuring a series of ϕ scans at various ψ angles it is possible to measure the 3-D orientational distribution of the plane normals (known as poles). To produce a 2-D representation of the 3-D distribution the poles which lie on the surface of a sphere may be projected onto the equatorial plane, producing a pole figure. Two common projections used in this work are the Schmidt projection and the Wulff projection.

The resolution in ϕ and ψ is limited by the optical arrangement. For a 0.45 mm receiving slit the instrumental broadening (FWHM) in degrees is [210]:

$$\delta\phi \approx 0.90 / \sin\psi \tag{3.10}$$

$$\delta\psi \approx 0.55 / \sin\theta \tag{3.11}$$

These are approximations which become inaccurate at small values of ψ and θ respectively but are correct in situations for which they will be used in this work. In order to verify that these estimates are reasonable an experiment has been carried out in which a {111} pole figure of an MgO single crystal is measured. We can assume that this sample has a peak width which is negligible in comparison with the instrumental broadening. Therefore, the poles observed will have FWHM approximately equal to the instrumental broadening in the ϕ and ψ directions. The (111) pole is measured at a value of 2θ=38.9° and ψ=55°. Equations 3.10 and 3.11 are used to calculate the values in table 3.2, which are compared with those measured experimentally.

Table 3.2 Calculated and measured instrumental broadening of the {111} poles of MgO

	Calculated FWHM (°)	Measured FWHM (°)
$\delta\phi$	1.10	1.2 ± 0.1
$\delta\psi$	1.74	1.7 ± 0.1

Note that the experiment has been carried out with different widths of receiving slits and no significant change to the broadening of these peaks is observed.

3.4 Other Characterisation Methods

3.4.1 Film surface analysis

The surfaces of films and tapes have been investigated using reflected light microscopy, atomic force microscopy and stylus profilometry. The optical microscope used has a resolution of approximately 1 μm. For higher resolution images of the sample surface (of around 10 nm), an atomic force microscope (AFM) (Digital Instruments Nanoscope III) has been used in tapping mode. A sharp probe tip mounted on a flexible cantilever scans across the specimen surface. The cantilever is vibrated and when brought close to the specimen the tip interacts with the atoms on the surface. The tip height is then adjusted using a piezoelectric crystal in order to maintain a constant vibrational amplitude, which equates to a constant distance above the sample surface. Hence the surface topography can be elucidated from the voltage applied to the piezoelectric crystal as it is scanned across the surface. Surface profiles may also be obtained using a stylus profilometer, though the depth resolution is only around 50 nm. However it is useful for measuring step heights in order to determine film thicknesses.

3.4.2 Superconducting parameters

The critical transition temperature, T_c is measured using a standard 4 probe method. Current and voltage pins are placed in contact with the superconducting film and lowered into a helium dewar. The resistance is then measured as a function of temperature to determine T_c and the width of the transition.

Scanning Hall Probe measurements have been carried out using an array of 3 mutually perpendicular Hall probes [211]. As shown in figure 3.10 the array is held approximately 100 μm above the sample surface and scanned in a horizontal plane using stepper motors. A

magnetic field is ramped up to 0.8 T and back to zero in order to trap flux in the sample and set up shielding currents. The Hall Probe is then scanned across the surface in steps of 100 μm, and the 3 components of magnetic field measured.

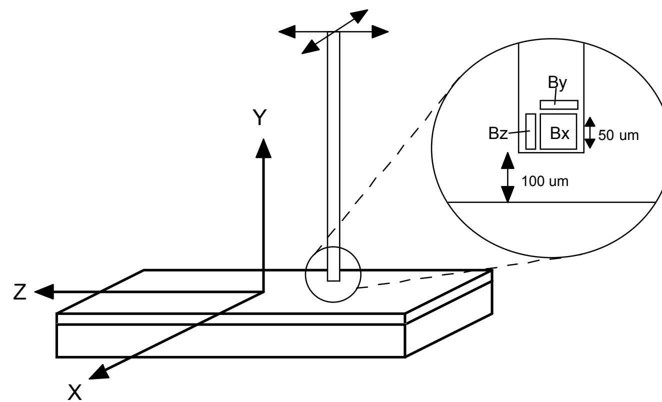

Figure 3.10 Hall Probe measurement apparatus

CHAPTER THREE **69**

EXPERIMENTAL TECHNIQUES **69**

3.1 AN INTRODUCTION TO THIN FILM DEPOSITION 69

3.1.1 The sputtering process *69*

3.1.2 Magnetrons *70*

3.1.3 RF sputtering *71*

3.1.4 Reactive sputtering *72*

3.1.5 Nucleation and growth *72*

3.1.6 Epitaxy *73*

3.2 PRACTICAL THIN FILM GROWTH 74

3.2.1 Vacuum systems *74*

3.2.2 Magnetrons and shields *75*

3.2.3 Targets *76*

3.2.4 Substrate heating *76*

3.2.5 Temperature measurement *78*

3.2.6 Deposition procedures *79*

3.3 X-RAY DIFFRACTION 80

3.3.1 The Ward-Wallace camera *80*

3.3.2 The vertical diffractometer *82*

3.3.1 The texture goniometer *84*

3.4 OTHER CHARACTERISATION METHODS 86

3.4.1 Film surface analysis *86*

3.4.2 Superconducting parameters *86*